Fabrication and Photoelectrochemical Characteristics of the Patterned CdS Microarrays on Indium Tin Oxide Substrates

Xu Meng,[†,‡] Yongjuan Lu,[†,§] Baoping Yang,[‡] Gewen Yi,*[,†] and Junhong Jia*[,†]

State Key Laboratory of Solid Lubrication, Lanzhou Institute of Chemical Physics, Chinese Academy of Sciences, Lanzhou, 730000 China, College of Petrochemical Technology, Lanzhou University of Technology, Lanzhou, 730050 China, and Graduate School of Chinese Academy of Sciences, Beijing 10049, China

ABSTRACT In an effort to investigate the extraordinary photoelectrochemical characteristics of nanostructured CdS thin films in promising photovoltaic device applications, the patterned CdS microarrays with different feature sizes (50, 130, and 250 μm in diameter) were successfully fabricated on indium tin oxide (ITO) glass substrates using the chemical bath deposition method. The ultraviolet lithography process was employed for fabricating patterned octadecyltrichlorosilane (OTS) self-assembled monolayers (SAMs) as the functional organic thin layer template. The results show that the regular and compact patterned CdS microarrays had been deposited onto ITO glass surfaces, with clear edges demarcating the boundaries between the patterned CdS region and substrate under an optimal depositing condition. The microarrays consisted of pure nanocrystalline CdS with average crystallite size of about 10.7 nm. The photocurrent response and the optical adsorption of the patterned CdS microarray thin films increased with the decrease of the feature size, which was due to the increased CdS surface area, as well as the increased optical path length within the patterned CdS thin films, resulting from multiple reflection of incident light. The resistivity values increase with the increase of feature size, due to the increase of the relative amount of gaps between CdS microarrays with increasing the feature size of patterned CdS microarrays.

KEYWORDS: cadmium sulfide • thin film • micropattern • photoelectrochemical property

INTRODUCTION

Cadmium sulfide (CdS) is one of the promising n-type semiconductor materials for use in solar cell devices, thin film transistors for flat panel displays, optical filters, photodetectors, photovoltaics, and gas sensors (1−7). The nanotructured CdS thin films have attracted extensive attention in recent years, due to their widened industrial applications in many fields, especially for their interesting optical and optoelectronic properties for potential photovoltaic applications (8). Various techniques, such as vacuum evaporation (9), spray deposition, electrodeposition (10), screen printing (11), chemical vapor deposition, molecular beam epitaxy (12), and chemical bath deposition (CBD) (13−17) have been utilized to prepare CdS thin films. Among these methods, CBD is known to be a simple, no requirement for sophisticated instruments, low temperature, and convenient for large area deposition technique (18, 19). CBD is a slow process, which facilitates the better orientation of the crystallites with improved grain structure (3).

In recent years, studies of surface patterned and miniaturization techniques have created the need for controlling surface properties as well as other potential properties (20). Patterning techniques are very important for fabricating thin film devices and application in most microsystems for controlling the spatial position of functional materials, such as microelectronic, sensors, electrical and optical devices, microelectromechanical systems (MEMS), and photonic systems. There have been many breakthroughs in micro- and nanosized materials in light of the patterning techniques (21). Thus, in order to investigate innovative characteristics of CdS thin films, it may be necessary to control the spatial regulation through fabricating patterns. A number of patterning techniques, such as template-assisted atomic layer deposition, scanning probe lithography, microcontact printing, and femtosecond laser pulses, have been developed to fabricate patterned semiconductor thin films in microscale or nanoscale (22−26). Self-assembled monolayers (SAMs) have been used as templates to produce micro- and nanoscale patterned structures using a variety of techniques, including ultraviolet lithography (27), scanning probe lithographies (28), microcontact printing (29), and electron-beam patterning (30). Among these, the ultraviolet lithography is a simple, inexpensive, and practical technique. So far, there have been many reports on fabricating patterned thin films. Tokuhisa and co-workers (31) fabricated patterned TiO_2 thin films using polymer-on-polymer stamping of block copolymers as a template. Lee and co-workers (32) prepared patterned ZrO_2 thin films using photocatalytic lithography of the alkylsiloxane SAMs and selective atomic layer deposition (ALD). Lu and co-workers (33) successfully deposited positive and negative micropatterned copper sulfide thin films on patterned Si substrates with $-NH_2/-CH_3$ and $-NH_2/$

* Corresponding author. Tel.: +86-931-4968611 (J.J. and G.Y.). Fax: +86-931-8277088 (J.J. and G.Y.). E-mail: jhjia@licp.cas.cn (J.J.), gwyi@licp.cas.cn (G.Y.).
Received for review June 24, 2010 and accepted November 1, 2010
[†] Lanzhou Institute of Chemical Physics, Chinese Academy of Sciences.
[‡] Lanzhou University of Technology.
[§] Graduate School of Chinese Academy of Sciences.
DOI: 10.1021/am100548w

−OH different SAM terminated silane. Hwang and co-workers (29) fabricated micropatterned CdS thin films through selective solution deposition using microcontact printing techniques. Meldrum and co-workers (34) prepared patterned sulfide thin films (ZnS, PbS) in the same way. However, there are few reports on studying growth mechanisms of patterned CdS films as well as the effects of the patterning on its optical and photoelectrochemical properties.

In this work, we described a convenient, simple, inexpensive, and practical route for fabricating patterned CdS microarray thin films with different feature sizes (50, 130, and 250 μm) on indium tin oxide (ITO) glass substrates by the CBD deposition technique and using the ultraviolet lithographed octadecyltrichlorosilane (OTS) SAMs as the functional organic thin layer template. The characterization and photoelectrochemical properties of the patterned CdS microarrays, along with the effects of the pattern features on the optical and photoelectrochemical properties of patterned thin films were investigated. The growth mechanisms of CdS on the patterned SAMs with different functionalized terminal groups were also discussed. It is expected that this method can be used to effectively regulate the surface feature size as well as photoelectrochemical properties of CdS thin films.

EXPERIMENTAL SECTION

Materials and Reagents. Analytical-grade cadmium acetate ($Cd(CH_3COO)_2 \cdot 2H_2O$), triethanolamine ($N(CH_2CH_2OH)_3$, TEA), and thiourea ($H_2NCSNH_2$) with purities better than 98% were purchased commercially and used as received. Octadecyltrichlorosilane (OTS, 95%) was purchased from Aldrich. All chemicals were used without further purification.

The substrates used in the present study were ITO glass, cut into 1 × 2 cm^2 pieces for CdS deposition. Prior to film deposition, the substrates were ultrasonically cleaned by soaking in deionized water, acetone, and isopropyl alcohol, respectively, followed by thorough rinsing with deionized water and drying with dry nitrogen.

Fabrication of Patterned CdS Microarrays. Figure 1 presents a schematic of the fabrication processes of patterned SAMs similar to that reported in our previous work (33). The patterned SAMs with $-NH_2/-CH_3$ and $-NH_2/-OH$ terminated silane on ITO glass substrate were prepared in a similar manner. The $-CH_3/-OH$ SAMs microarray patterns with different feature sizes could be produced using different masks with feature sizes of 50, 130, and 250 μm, respectively.

The substrates with $-CH_3/-OH$ SAMs microarray patterns were immersed in an aqueous solution of cadmium acetate, thiourea, and triethanolamine (TEA, complexing agent) in alkaline media. The deposition time and temperature depended on the bath solution compositions. The substrates were placed vertically to the bottom of the beakers to avoid the effect of gravity. The deposited films were rinsed with deionized water and ultrasonically washed in isopropyl alcohol to remove the leftover CdS nanoparticles and then dried with a nitrogen gas flow. Meanwhile, the patterned microarrays with different features were deposited synchronously in the same aqueous solution and deposition time in one pot to avoid the film thickness differences.

Characterization. The surface morphologies of the patterned CdS microarrays were examined using a JSM-5600LV scanning electron microscope (SEM, Japan) and a Micro-XAM 3D Surface Profiler (Micro-XAM, USA). In order to increase the resolution of SEM observations, the tested composite specimens were

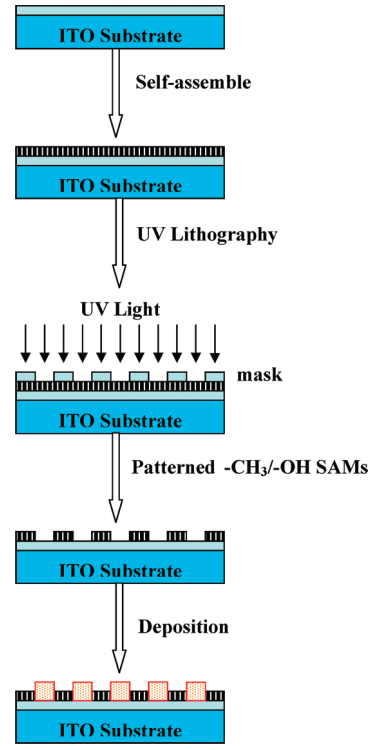

FIGURE 1. Schematic diagrams of the fabrication process for patterned CdS microarrays.

plated with a gold coating to render the electric conductivity. The structure and the phase composition were analyzed by X'pert PRO X-ray diffraction (XRD, Netherlands) with Cu Kα radiation (λ = 1.5406 Å) at a scanning speed of 1.2°/min. The chemical states of the elements on the films were determined using a PHI5702 multifunctional X-ray photoelectron spectroscope (XPS, USA). XPS analysis was conducted at 400 W and pass energy of 29.35 eV, using Al Kα (1486.6 eV) radiation as the excitation source, and the binding energy of contaminated carbon (C1s = 284.6 eV) was used as reference. The optical absorption was measured by a Spect-50 UV−vis spectrophotometer (Jena, Germany) in the wavelength range of 280−1000 nm. The photoelectric response was measured using a electrochemical workstation (CHI660d, China) with a three-electrode system, in which patterned CdS thin film, a platinum wire, and saturation calomel electrode were used as the working electrode, the counter electrode, and reference electrode, respectively. A 125 W UV mercury lamp (λ = 365 nm) was used as the light source. The electrolyte, aqueous $HClO_4$ (0.1 mol/L) solution, was freshly prepared using double deionized water. Electrical properties were performed using a four-point probe resistivity measurement instrument (KDY-1, China).

RESULTS AND DISCUSSION

Surface Morphological Analysis. The successful synthesis of patterned CdS microarrays on ITO glass substrate required the optimization of the synthesis parameters such as concentrations of precursors and complexing agent, pH value, and deposition temperature. Such parameters were systematically varied as summarized in Table 1. After a series of experiments, the optimum conditions for thin film formation were found to be a concentration of Cd^{2+} of 0.01 mol/L, [TEA]/[Cd] ratio of 2, pH of 10.0−10.5, and temperature of about 70 °C. The clearly defined CdS patterns with compact and uniform CdS nanoparticles can be obtained under the optimal depositing condition.

Table 1. Deposition Conditions of Patterned CdS Thin Films

No.	$Cd(CH_3COO)_2 \cdot 2H_2O$, mol/L	$(NH_2)_2CS$, mol/L	$N(CH_2CH_2OH)_3$, mol/L	temperature, °C	pH
A	[Cd]/[S-urea]/[TEA] = 1/1/1			70	10.0−10.5
B	[Cd]/[S-urea]/[TEA] = 1/1/2			70	10.0−10.5
C	[Cd]/[S-urea]/[TEA] = 1/1/3			70	10.0−10.5
D	0.01	0.01	0.02	70	8.5−9.0
E	0.01	0.01	0.02	70	10.0−10.5
F	0.01	0.01	0.02	70	11.0−11.5
G	0.01	0.01	0.02	60	10.0−10.5
H	0.01	0.01	0.02	70	10.0−10.5
I	0.01	0.01	0.02	80	10.0−10.5
J	0.01	0.01	0.02	90	10.0−10.5
K	0.0025	0.0025	0.005	70	10.0−10.5
L	0.005	0.005	0.01	70	10.0−10.5
M	0.01	0.01	0.02	70	10.0−10.5
N	0.04	0.04	0.08	70	10.0−10.5

The SEM micrographs allow us to obtain information about the microstructure of sample surfaces. Figure 2 shows the micrographs of patterned CdS microarrays with different feature sizes (50, 130, and 250 μm) on the ITO glass substrates. As expected, regular and compact patterns with high resolution and consistently high quality pattern geometry were obtained. The bright areas corresponded to the dense growth of cadmium sulfide nanocrystalline on the SAMs with −OH end groups. The boundary between the cadmium sulfide patterns and the hydrophobic areas (OTS-SAMs) were sharply demarcated and could be clearly visible. Two regions of in-circle regions (cadmium sulfide patterns) and out-circle regions (OTS-SAMs) display a dramatic contrast in morphology. The crystals grown in the −OH-terminated (in-circle) regions are dense, compact, continuous, and well-adhered on the ITO glass substrate even after sonication. While on the $-CH_3$-terminated (out-circle) regions, there is almost no cadmium sulfide nanocrystalline.

The morphologies and the height profiles of patterned CdS microarrays on the ITO glass surface with different feature sizes were also characterized using 3D Surface

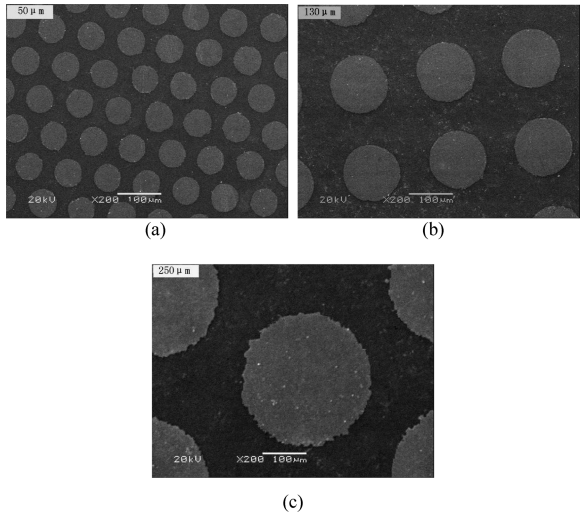

FIGURE 2. SEM images of circular-patterned CdS microarrays on the ITO glass surface with different feature sizes: (a) 50 μm, (b) 130 μm, and (c) 250 μm.

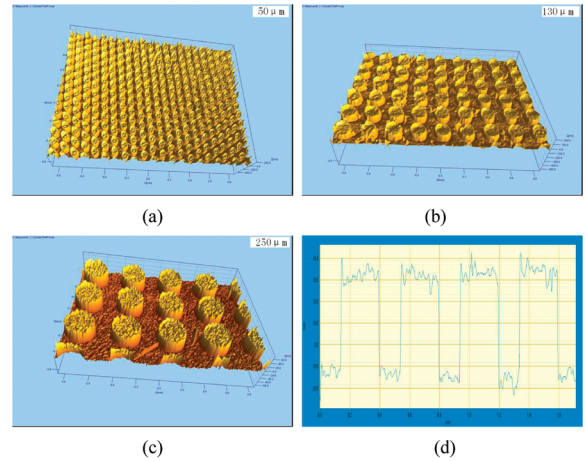

FIGURE 3. 3D surface images of patterned CdS microarrays on the ITO glass surface with different feature sizes: (a) 50 μm, (b) 130 μm, (c) 250 μm, and (d) height profile.

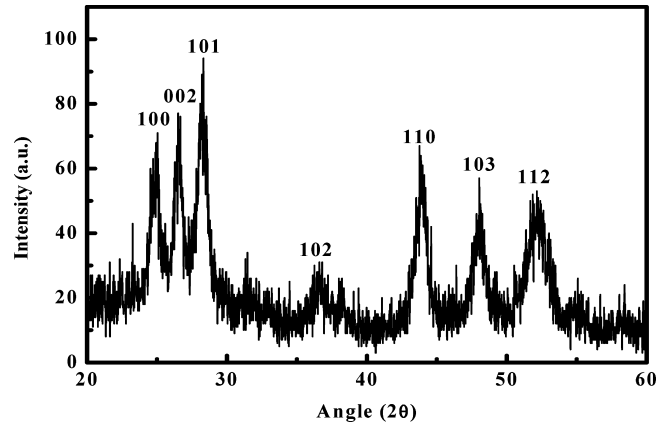

FIGURE 4. XRD pattern of the CdS thin film.

Profiler. As showed in Figure 3, the microscopic structure of the patterned cadmium sulfide microarrays consisted of columnar microarrays on the ITO substrates. The patterns are regular over a large area and have relatively clear boundaries, and the column height (i.e., thickness of cadmium sulfide thin film) is about 40 nm.

X-ray Diffraction and Compositional Analysis. The XRD measurements of the CdS patterns without ion beam sputtering were also carried out as shown in Figure 4. The diffraction peaks, appearing at the diffraction angles of 25.0°, 26.7°, 28.3°, 43.8°, 48.1°, and 52.1°, can be indexed to the diffraction angles of the crystal face of (100), (002), (101), (110), (103), and (112) of hexagonal CdS (JCPDS 80-0006). It indicates that the CdS is composed of single-phase crystallite without impurity. The XRD pattern shows a strong peak at $2\theta = 28.3°$; it implies the preferentially oriented crystals with the [101] direction. The crystallite size of CdS was calculated using the Scherrer's relation (35).

$$d = \frac{0.9\lambda}{\beta \cos \theta}$$

where β is the broadening of diffraction line measured at half-maximum intensity (radians) and $\lambda = 1.5406$ Å, the

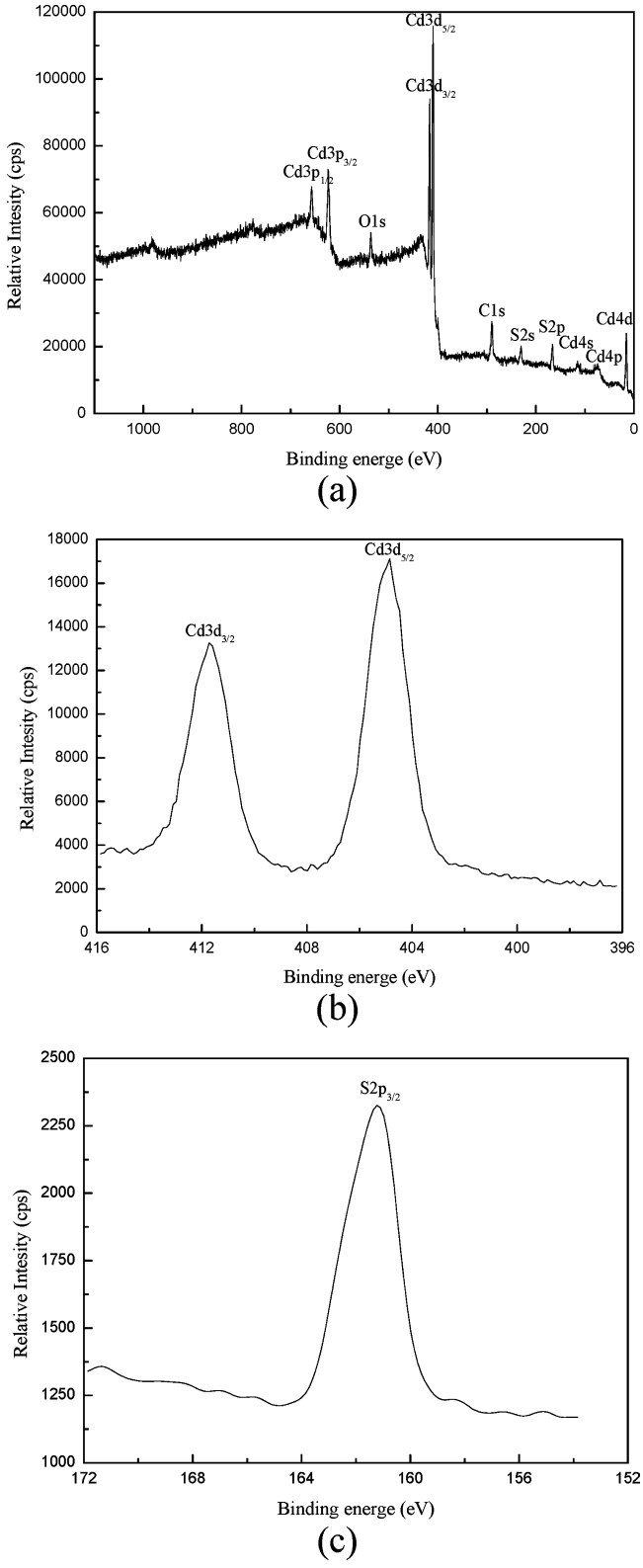

FIGURE 5. XPS spectrum of the CdS patterns: (a) typical XPS survey spectrum of the CdS patterns, (b) core level spectrum for Cd3d, (c) core level spectrum for S2p.

wavelength of Cu Kα. The average crystallite size was calculated to be about 10.7 nm.

Surface states of elements of the patterned CdS microarrays were studied using an X-ray photoelectron spectroscope. Figure 5 shows the typical XPS survey spectrum and high-resolution spectrum values of Cd3d and S2p peaks in this study. The spectrum confirmed the high chemical purity of the CdS nanoparticles consisted solely of Cd and S (the carbon content and the C 1s line shape were typical of surface contamination detected in air-exposed oxide surfaces). The peaks of the binding energies of 404.9 and 411.7 eV were assigned to Cd in CdS (Figure 5b), and 161.2 eV was assigned to S in CdS (Figure 5c). Thus, the XPS spectrum further confirmed that the CdS patterns were composed of pure CdS nanocrystalline.

Nucleation and Growth Mechanism of Patterned Microarrays. According to the DLVO (Derjaguin, Landau, Verwey, and Overbeek) theory (36), the total energy between the interacting surfaces can be divided into three parts: electrostatic interactions, London–van der Waals interactions (always attractive), and hydration interaction (always repulsive). Usually, the electrostatic is the dominant factor during chemical bath deposition (CBD) (33). Solution chemistry greatly affects films formation. Nucleation can take place in the solution (homogeneous) or on the substrate surface (heterogeneous). The physical properties of films change due to the degree of supersaturation, interfacial energy, and the strength of coordination bonds of the chelating reagents. The growth mechanism of samples was discussed using the stability of metal complexes and classical nucleation theory (37).

The SAMs on substrate surfaces provide an environment to investigate the influences of surface properties on nucleation of solids from liquid phases. $-CH_3$/$-OH$ SAMs microarray patterns provided the major difference of the surface functionality after the OTS-SAMs surface through masks with different feature sizes under a UV light. UV-irradiation causes the formation of silanol groups (Si$-$OH) in the exposed areas, the nonirradiated regions, which retain the structure of the native SAMs ($-CH_3$-terminated groups).

The SAMs of silanol groups (Si$-$OH) enhance the chemical affinity with cadmium sulfide, resulting in a decrease in the interfacial tension, which promotes the heterogeneous nucleation on the surface. The SAMs of $-CH_3$-terminated regions should have no electrostatic interaction with cadmium sulfide nanoparticles with negative charges. Although a few cadmium sulfide nanoparticles attached onto the $-CH_3$-terminated surface due to the van der Waals interactions, they can be easily washed off from the surface by ultrasonication. The production of CdS nanocrystalline from thiourea and a water-soluble cadmium salt in an alkaline ammonia medium can be written as follows (38):

$$Cd(NH_3)_n^{2+} + (NH_2)_2CS + 2OH^- \rightarrow CdS + nNH_3 + H_2NCN + 2H_2O$$

The CBD is based on the formation of solid phase from a solution, which involves two steps as nucleation and particle growth. Homogeneous nucleation to form CdS thin films begins on the formation of CdS nucleus onto the surface of the substrate, the step followed by particle growth until particular thickness (35).

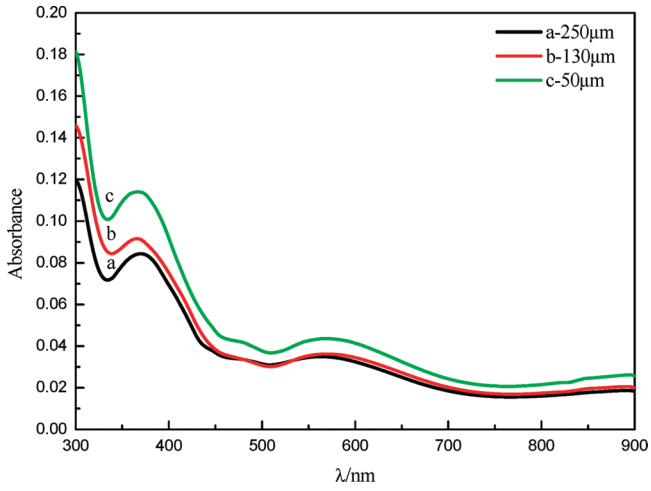

FIGURE 6. UV−vis absorption spectrum of patterned CdS microarrays with different feature sizes: (a) 250 μm, (b) 130 μm, and (c) 50 μm.

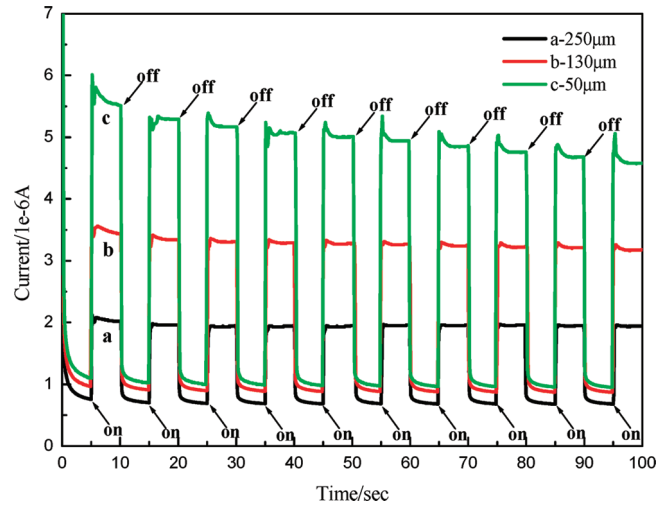

FIGURE 7. Photocurrent response spectrum of patterned CdS microarray electrodes with different feature sizes under the on−off UV light illumination: (a) 250 μm, (b) 130 μm, and (c) 50 μm.

Optical Properties. It is well-known that the CdS thin films have a very strong absorption in the ultraviolet range (39). Figure 6 shows the UV−vis adsorption spectrum of three patterned CdS microarray thin films with different feature sizes on ITO glass substrates. It can be seen that the patterned CdS microarray thin films with different feature sizes had different absorptions in the ultraviolet range, and the absorbance intensity increased with the increase of the density of discrete CdS domains. This enhancement in the absorbance intensities could be attributable to the following three reasons (40): (a) the surface area of CdS increases with an increase of the density of CdS domains, which leads to higher absorption; (b) the total optical path length within the patterned CdS microarrays would also increase with an increase of the density of CdS domains; (c) surface tailoring enabling effective light trapping properties, it has to scatter the incident light efficiently leading to an effective light trapping inside the CdS thin film layers, a longer traveling path of photons in the patterned CdS thin films that causes more optical absorption. These results indicate that the feature size of the CdS patterns can effectively affect the UV−vis absorption performance of the patterned CdS thin films.

Photoelectrochemical Properties. To understand the photoelectrochemical properties of the synthesized patterned CdS microarrays, photocurrent measurements have been performed in a photoelectrochemical cell containing a 0.1 mol/L aqueous solution of perchloric acid ($HClO_4$) and illuminated with a 125 W UV mercury lamp ($\lambda = 365$ nm). The photocurrent response spectrum of the patterned CdS microarrays with different feature sizes are shown in Figure 7. A strong photocurrent response was observed for patterned CdS microarrays and described the typical characteristic of n-type semiconductor materials. That is, the n-type semiconductor will release electron under the light illumination and increase the amount of electron passes to the outer electric circuit, resulting in an increase of photocurrent value (35).

Furthermore, it can be seen that the photocurrent decreased with an increase of the feature size of the CdS patterns. When the UV light was regularly switched on and off, a series of almost identical electric signals could be obtained and hold the stable photocurrent. For the patterned CdS microarrays with different feature sizes of 50, 130, and 250 μm, the generated photocurrents were 5.5, 3.5, and 2×10^{-6} A, respectively. The peak photocurrent of the patterned CdS thin film electrodes undergoes a gradual increase with the decrease of the feature sizes. This enhancement not only is due to an increase of the surface area of the patterned CdS thin films but also may be due to the photonic enhancement or an increased optical path length within the CdS microarray patterns with a smaller feature size, resulting from multiple reflection of incident light, which might lead to enhanced photocurrent generation (40). In any case, that photocurrent generation is highly dependent on the CdS pattern feature sizes, and the patterning technology is an effective method for controlling the surface and photoelectrochemical properties. Such patterned structures can be used to direct the assembly of other functional materials and fabrication of patterned film with feature size in submicroscale, and the scale effects on the photoelectrochemical properties remain a further investigation in the succeeding research.

Electrical Properties. Figure 8 presents the typical *V*/*I* characteristics of patterned CdS microarrays with different feature sizes. The *V*/*I* characteristics are linear indicating the Ohmic contact of electrodes with patterned CdS thin films (41). The voltage values are different for patterned CdS microarrays with different feature sizes. The voltage values will increase with the increase of feature size at the same current value, i.e., the resistivity values increase with the increase of feature size. The difference is due to the decrease of the density of CdS domains with a larger feature size. Increasing the feature size of patterned CdS microarrays results in the increase of the relative amount of gaps between CdS microarrays and, therefore, reduces the conductivity.

CONCLUSIONS

The patterned CdS microarrays with different feature sizes (50, 130, and 250 μm) on ITO glass substrates were

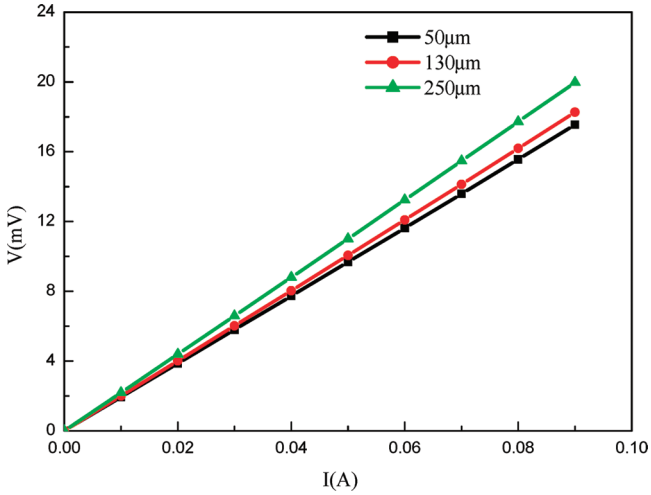

FIGURE 8. *V/I* characteristic spectrum of patterned CdS microarray electrodes with different feature sizes: (a) 50 μm, (b) 130 μm, and (c) 250 μm.

successfully fabricated by a chemical bath deposition technique combined with the ultraviolet lithography method using OTS SAMs as the functional organic thin layer template. The SEM and 3D Surface Profiler images showed that the high selectivity and sharp boundaries patterned CdS thin films with uniform, compact CdS nanoparticles can be obtained using the CBD techniques under the optimal depositing condition. The XRD and XPS studies confirmed that the patterned microarrays consisted of nanocrystalline CdS with average crystallite size of about 10.7 nm. The characteristic UV−vis spectrum and photocurrent response spectrum demonstrated that these properties were dependent on the feature sizes of the CdS patterns. The photocurrent response of the patterned CdS thin films increased with the decrease of the feature size, which was due to the increased CdS surface area as well as the increased optical path length within the patterned CdS thin films, resulting from multiple reflection of incident light. The resistivity values increase with the increase of feature size, due to the increase of the relative amount of gaps between CdS microarrays with an increase in the feature size of patterned CdS microarrays. This work indicates that patterned CdS thin films are attractive systems for surface tailoring and also provide a novel method to effectively control the photoelectrochemical properties of nanostructured CdS thin films with promising applications in microsystem devices.

Acknowledgment. The authors gratefully acknowledge the National Natural Science Foundation of China (Grant Nos. 50705094, 50972148) and the "Hundred Talents Program" of Chinese Academy of Sciences (Grant No. KGCX2-YW-804) for providing the financial support.

REFERENCES AND NOTES

(1) Bilgin, V.; Kose, S.; Atay, F.; Akyuz, I. *Mater. Chem. Phys.* **2005**, *94*, 103–108.
(2) Mendoza-Perez, R.; Santana-Rodriguez, G.; Sastre-Hernandez, J.; Morales-Acevedo, A.; Arias-Carbajal, A.; Vigil-Galan, O.; Alonso, J. C.; Contreras-Puente, G. *Thin Solid Films* **2005**, *480*, 173–176.
(3) Prabahar, S.; Dhanam, M. *J. Cryst. Growth* **2005**, *285*, 41–48.
(4) Ximello-Quiebras, J. N.; Contreras-Puente, G.; Aguilar-Hernández, J.; Santana-Rodriguez, G.; Arias-Carbajal Readigos, A. *Sol. Energy Mater. Sol. Cells* **2004**, *82*, 263–268.
(5) Enriguez, J. P.; Mathew, X. *Sol. Energy Mater. Sol. Cells* **2003**, *76*, 313–322.
(6) Cetinorgu, E.; Gumus, C.; Esen, R. *Thin Solid Films* **2006**, *515*, 1688–1693.
(7) Zhang, H.; Ma, X. Y.; Yang, D. R. *Mater. Lett.* **2004**, *58*, 5–9.
(8) Hilal, H. S.; Ismail, R. M. A.; El-Hamouz, A.; Zyoud, A.; Saadeddin, I. *Electrochim. Acta* **2009**, *54*, 3433–3440.
(9) Mahmoud, S. A.; Ibrahim, A. A.; Riad, A. S. *Thin Solid Films* **2000**, *372*, 144–148.
(10) Premaratne, K.; Akuranthilaka, S. N.; Dharmadasa, I. M.; Samantilleka, A. P. *Renewable Energy* **2004**, *29*, 549–557.
(11) Al Kuhaimi, S. A. *Vacuum* **1998**, *51*, 349–355.
(12) Brunthaler, G.; Lang, M.; Forstner, A.; Giftge, C.; Schikora, D.; Ferreira, S.; Sitter, H.; Lischka, K. *J. Cryst. Growth* **1994**, *138*, 559–563.
(13) Kostoglou, M.; Andritsos, N.; Karabelas, A. J. *Thin Solid Films* **2001**, *387*, 115–117.
(14) Sankar, N.; Sanjeeviraja, C.; Ramachandran, K. *J. Cryst. Growth* **2002**, *243*, 117–123.
(15) Schon, J. H.; Schenker, O.; Batlogg, B. *Thin Solid Films* **2001**, *385*, 271–274.
(16) Contreras, M. A.; Romero, M. J.; Hasoon, B. T. E.; Noufi, R.; Ward, S.; Ramanathan, K. *Thin Solid Films* **2002**, *403*, 204–211.
(17) Martinez, M. A.; Guillen, C.; Herrero, J. *Appl. Surf. Sci.* **1999**, *140*, 182–189.
(18) Sasikala, G.; Thilakan, P.; Subramanian, C. *Sol. Energy Mater. Sol. Cells* **2000**, *62*, 275–293.
(19) Hiie, J.; Dedova, T.; Valdna, V.; Muska, K. *Thin Solid Films* **2006**, *511*, 443–447.
(20) Amos, F. F.; Morin, S. A.; Streifer, J. A.; Hamers, R. J.; Jin, S. *J. Am. Chem. Soc.* **2007**, *129*, 14296–14302.
(21) Lu, P.; Walker, A. V. *ACS Nano* **2009**, *3*, 370–378.
(22) Xu, D. W.; Graugnard, E.; King, J. S.; Zhong, L. W.; Summers, C. J. *Nano Lett.* **2004**, *4*, 2223–2226.
(23) Wang, X. D.; Neff, C.; Graugnard, E.; Ding, Y.; King, J. S.; Pranger, L. A.; Tannenbaum, R.; Wang, Z. L.; Summers, C. J. *Adv. Mater.* **2005**, *17*, 2103–2106.
(24) Passinger, S.; Saifullah, M. S. M.; Reinhardt, C.; Subramanian, K. R. V.; Chichkov, B. N.; Welland, M. E. *Adv. Mater.* **2007**, *19*, 1218–1221.
(25) Nelson, J. B.; Schwartz, D. T. *Langmuir* **2007**, *23*, 9661–9666.
(26) Shirahata, N.; Sakka, Y.; Hozumi, A. *Thin Solid Films* **2006**, *499*, 293–298.
(27) Brewer, N. J.; Rawsterne, R. E.; Kothari, S.; Leggett, G. J. *J. Am. Chem. Soc.* **2001**, *123*, 4089–4090.
(28) Gates, B. D.; Xu, Q. B.; Stewart, M.; Ryan, D.; Willson, C. G.; Whitesides, G. M. *Chem. Rev.* **2005**, *105*, 1171–1196.
(29) Hwang, Y. K.; Woo, S. Y.; Lee, J. H.; Jung, D. Y.; Kwon, Y. U. *Chem. Mater.* **2000**, *12*, 2059–2063.
(30) Whelan, C. S.; Lercel, M. J.; Craighead, H. G.; Seshadri, K.; Allara, D. L. *Appl. Phys. Lett.* **1996**, *69*, 4245–4247.
(31) Tokuhisa, H.; Hammond, P. T. *Langmuir* **2004**, *20*, 1436–1441.
(32) Lee, J. P.; Sung, M. M. *J. Am. Chem. Soc.* **2004**, *126*, 28–29.
(33) Lu, Y. J.; Liang, S.; Chen, M.; Jia, J. H. *J. Colloid Interface Sci.* **2009**, *332*, 32–38.
(34) Meldrum, F. C.; Flath, J.; Knoll, W. *Thin Solid Films* **1999**, *348*, 188–195.
(35) Puspitasari, I.; Gujar, T. P.; Jung, K. D.; Joo, O. S. *J. Mater. Process. Technol.* **2008**, *201*, 775–779.
(36) Shin, H.; Agarwal, M.; De Guire, M. R.; Heuer, A. H. *Acta Mater.* **1998**, *46*, 801–815.
(37) Chang, C. C.; Liang, C. J.; Cheng, K. W. *Sol. Energy Mater. Sol. Cells* **2009**, *93*, 1427–1434.
(38) Kozhevnikova, N. S.; Rempel, A. A.; Hergert, F.; Magerl, A. *Thin Solid Films* **2009**, *517*, 2586–2589.
(39) Ravichandran, K.; Philominathan, P. *Appl. Surf. Sci.* **2009**, *255*, 5736–5741.
(40) Chen, D.; Gao, Y. F.; Wang, G.; Zhang, H.; Lu, W.; Li, J. H. *J. Phys. Chem. C* **2007**, *111*, 13163–13169.
(41) Xin, M. D.; Li, K. W.; Wang, H. *Appl. Surf. Sci.* **2009**, *256*, 1436–1442.

AM100548W